Beam tracing technique applied to LH wave propagation in tokamaks

N. Bertelli[1], O. Maj[2], E. Poli[2], R. Harvey[3], J. C. Wright[4], P. T. Bonoli[4],
C. K. Phillips[1], A. P. Smirnov[5], E. Valeo[1], J. R. Wilson[1],
[1] *Princeton Plasma Physics Laboratory, Princeton, NJ 08543, USA*
[2] *Max-Planck-Institut für Plasmaphysik, EURATOM Association, Garching, Germany*
[3] *CompX, Del Mar, CA 92014, USA*
[4] *MIT Plasma Science and Fusion Center, Cambridge, Massachusetts 02139, USA*
[5] *Lomonosov Moscow State University, Moscow, Russia*

Introduction. Lower hybrid current drive (LHCD) is a promising tool for current profile control in reactor grade plasmas. Some unresolved issues in the study of LH wave propagation still exist, such as the spectral gap problem [1] and, more recently, one related to the "density limit" in the efficiency of LHCD [2]. The most common approach used previously to analyze LH wave propagation is the ray tracing (RT) method based on the WKB approximation. Such a method, however, neglects wave diffraction effects and has applicability limitations in the cut-off and caustic regions which, in the multi-pass regime of the LH wave, can play an important role in determining the power absorption profile. These kind of limitations motivated the development of full-wave solvers like the `TORIC-LH` [3] and the `LHEAF` [4] codes. In this work, we make use of the beam tracing method based on the paraxial WKB (pWKB) approximation [5], which takes into account the effects of wave diffraction and yet retains all the numerical advantages of RT. A new modular version of the `LHBEAM` code [6, 7], which includes linear electron Landau damping and the reconstruction of the electric field, is presented. Some `LHBEAM` calculations and a comparison with the ray tracing code `GENRAY` [8] and the full wave solver `TORIC-LH` are also discussed.

LHBEAM: pWKB code for LH wave beam propagation. `LHBEAM` solves a set of ordinary differential equations, based on the pWKB approximation, for evolution of the wave beam taking into account diffraction effects. Specifically, the main equations describe [5]

- the evolution of the beam axis via the Hamiltonian equations of RT;
- the evolution of a symmetric complex matrix $\bar{s}_{ik} \equiv s_{ij} + i\phi_{ij}$ (summation over repeated indices is adopted),

$$\frac{d\bar{s}_{ij}}{d\tau} = -\frac{\partial^2 H}{\partial x^i \partial x^j} - \frac{\partial^2 H}{\partial x^j \partial N_k}\bar{s}_{ik} - \frac{\partial^2 H}{\partial x^i \partial N_k}\bar{s}_{jk} - \frac{\partial^2 H}{\partial N_k \partial N_l}\bar{s}_{ik}\bar{s}_{jl}, \tag{1}$$

  where s_{ij} and ϕ_{ij} are related to the phase front and the intensity profile of the beam cross-section, respectively; x^i and N_i are the components of the position vector $\mathbf{r}$ and the

refractive index $\mathbf{N}$, respectively. H is the (real) determinant of the dispersion tensor $\mathbf{\Lambda} = (\mathbf{NN} - N^2\mathbf{I}) + \boldsymbol{\varepsilon}^h$ ($\boldsymbol{\varepsilon}^h$ being the Hermitian part of the plasma dielectric tensor computed in the cold plasma limit and in the range of LH frequency approximation $\omega_{\rm ci}^2 \ll \omega^2 \ll \omega_{\rm ce}^2$);

- the wave energy transport: $\nabla \cdot (\mathbf{v}_g U) = -2\gamma U$ where $\mathbf{v}_g$ is the group velocity, U is the wave energy density and γ is the absorption coefficient.

The absorbed power is calculated according to the equation $\frac{dP}{d\tau} = -2\alpha_{\rm ELD} \left|\frac{\partial H}{\partial \mathbf{N}}\right| P$ where $d/d\tau \equiv \frac{\partial H}{\partial \mathbf{N}} \cdot \frac{d}{d\mathbf{r}}$ and $\alpha_{\rm ELD}$ denotes linear electron Landau damping given by

$$\alpha_{\rm ELD} = \frac{\gamma}{|\mathbf{v}_g|} = 2\sqrt{\pi}\left(\frac{\omega_{\rm pe}}{\omega}\right)^2 \frac{\omega}{c}\frac{c^3}{N_\parallel^3 v_{\rm th}^3}\left[(S-N_\parallel^2)(S-N^2)-D^2\right]\left|\frac{\partial H}{\partial \mathbf{N}}\right|^{-1} \exp\left[-\frac{c^2}{v_{\rm th}^2 N_\parallel^2}\right]. \quad (2)$$

In Eq. (2), $\omega_{\rm pe}$ is the electron plasma frequency, S and D are the components of the cold dielectric tensor in the Stix's notation [9], $N_\parallel$ is the parallel component of the refractive index with respect to magnetic field, c and $v_{\rm th} \equiv \sqrt{2T_{\rm e}/m_{\rm e}}$ are the speed of light and the electron thermal velocity, respectively. Furthermore, `LHBEAM` can reconstruct the wave electric field in both physical and Fourier space; the user can choose between an analytical and equilibrium prescribed numerically and between the full electromagnetic or the electrostatic dispersion relation.

Results and comparisons. Equilibrium and plasma parameters adopted in this work are typical of LH experiment in the Alcator C device, with a major radius $R_0 = 64$ cm and a minor radius $a = 16.5$ cm. The magnetic field is $B(R_0) = 8$ T and the plasma current is $I_{\rm p} = 400$ kA. The magnetic equilibrium is provided by a data file generated by the `ACCOME` code [10]. Temperature and density profiles are parabolic. The central and the edge electron density are $n_{\rm e,0} = 5 \times 10^{19}$ m^{-3} and $n_{\rm e,edg} = 1 \times 10^{19}$ m^{-3}. We consider three different values for the central electron temperature, namely, $T_{\rm e,0} = 3, 5, 10$ keV, whereas the edge electron temperature, for all three cases, is $T_{\rm e,edg} = 0.5$ keV. The initial conditions for the LH wave beam used for this specific analysis are such that the beam widths are $W_1 = 2.7$ cm and $W_2 = 0.4$ cm and the initial wave front of the LH beam is considered flat. Finally, the frequency of LH beam is 4.6 GHz and the initial value of the parallel refractive index on the beam axis is $N_{\parallel,0} = 2.5$, assuming a poloidal mode number $n_\theta = 0$. The input power is assumed to be 1 MW and the full electromagnetic dispersion function is adopted.

In Figure 1(a) we show a comparison between the poloidal projection of the wave beam propagation obtained from `LHBEAM`, represented by the shaded area with the poloidal projection of a bundle of rays generated by the RT code `GENRAY`, represented by the dashed lines. The solid (red) line refers to the beam axis. The spatial wave beam broadening originated by diffraction effects is very significant and completely missing in the RT description [6]. Figure 1(a) also

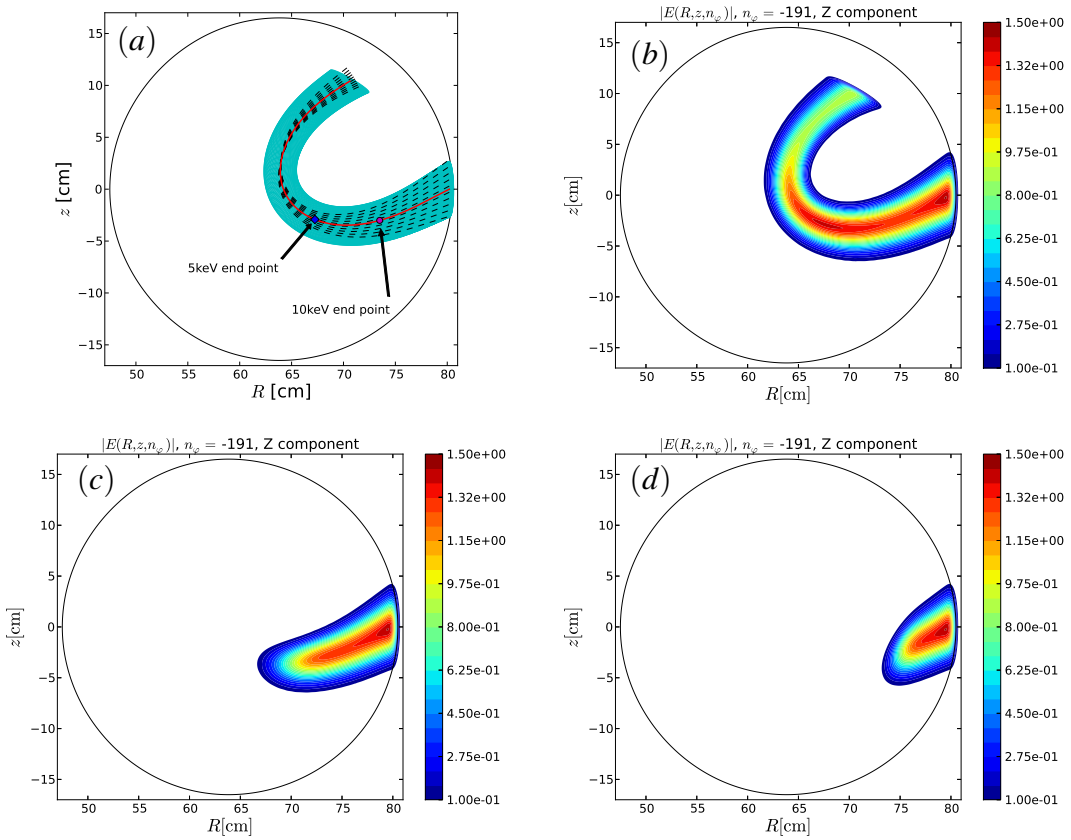

Figure 1: (a) Comparison between pWKB and ray tracing methods projected onto the poloidal cross-section. (b-d) Magnitude of the parallel component of the complex electric field normalized to its value at the launching point of the reference ray for three different cases: $T_{e,0} = 3$ keV (figure (b)), 5 keV (figure (c)), 10 keV (figure (d)), for the fixed toroidal mode number $n_\varphi = -191$, which corresponds to the dominant component of the spectrum.

shows the positions along the wave beam at which the power is fully absorbed for $T_{e,0} = 5$ keV (shown with a solid (blue) diamond) and 10 keV (shown with a solid (red) circle).

In the pWKB method, the solution for the wave field is directly obtained in the physical space. Therefore, in order to represent the wave electric field in the same way as that obtained from a spectral full wave solver, like `TORIC-LH`, which typically consider only a single toroidal Fourier mode n_ϕ, we have performed a Fourier transform of the electric field in the toroidal angle ϕ and we have selected the dominant component in the n_ϕ-spectrum. The results, for the magnitude of the parallel component of the complex electric field (normalized to the value of the total electric field amplitude at the launching point of the reference ray), are shown for $T_{e,0} = 3$ keV (figure 1(b)), $T_{e,0} = 5$ keV (figure 1(c)), and $T_{e,0} = 10$ keV (figure 1(d)). Comparing Figure 1(a) with Figure 1(b), one can see that the parallel component of the electric field follows very well the beam trajectory and its maximum lies on the beam axis and decreases away from it.

The absorbed power density profile is compared in Figure 2 with results from GENRAY and the full wave code TORIC-LH. Specifically, Figure 2 shows the power density as a function of the square root of the normalized poloidal flux, ρ_ψ. Three cases are shown for different central electron temperature, namely, $T_{e,0} = 3$ keV (red curves), $T_{e,0} = 5$ keV (green curves) and $T_{e,0} = 10$ keV (black curves) by using the circular cross-section equilibrium and the parabolic profiles described above. Solid, dashed and dashed-dotted lines correspond to LHBEAM, TORIC-LH and GENRAY results, respectively. From Figure 2, the results appear to be in good agreement. In particular, for $T_{e,0} = 5$, 10 keV, the results are very similar. It is worth noting that in the $T_{e,0} = 3$ keV case a reflection occurs at the plasma edge, because the power is not fully absorbed in a single pass. Therefore, $T_{e,0} = 3$ keV corresponds to a limit case for LHBEAM, as reflections are not yet treated explicitly in LHBEAM. Nonetheless, the agreement between the pWKB approximation and the full wave approach is quite good. Slight differences appear between LHBEAM and TORIC-LH, possibly because of the combined effects of the missing small amount of absorbed power after the reflection of the LH wave beam at the edge and the spatial dispersion in Eq. (2), which may require a specific treatment. The differences with GENRAY can be explained as the lack of the RT model to describe full wave effects such as diffraction. This is clearly shown in Figure figure 1(a) where pWKB technique shows a significant spatial broadening with respect to the RT method.

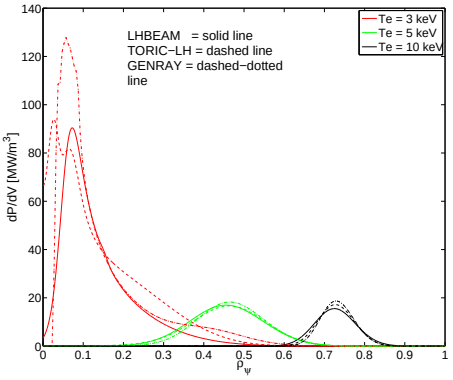

Figure 2: Power absorption profile versus the square root of the normalized poloidal flux.

Acknowledgments. This research is supported by the U.S. Department of Energy under contract number DE-FC02-99ER54512.

References

[1] P. T. Bonoli and R. C. Englade, Phys. Fluids **29**, 2937 (1986)
[2] G. Wallace et al., Phys. Plasmas **17**, 082508 (2010)
[3] J. C. Wright et al., Phys. Plasmas **16**, 072502 (2009)
[4] O. Meneghini et al., Phys. Plasmas Vol. 16, 090701 (2009)
[5] G. V. Pereverzev, Phys. Plasmas **5**, 3529 (1998)
[6] N. Bertelli, G. V. Pereverzev and E. Poli E, 34th EPS Conf. on Plasma Phys. **31F** P5.051 (2007)
[7] N. Bertelli et al., AIP Conference Proceedings **1069**, pp. 259-264 (2008)
[8] A. P. Smirnov and R. Harvey, Bull. Am. Phys. Soc. **40**, 1837 (1995)
[9] T. H. Stix, Waves in Plasmas, American Institute of Physics, NY, 1992
[10] R. S. Devoto et al., Nucl. Fusion **32**,773 (1992)